EUCLIPSE

EU Cloud Intercomparison, Process Study & Evaluation Project

Grant agreement no. 244067

Deliverable D3.3 Detailed analyses of the LES and SCM results for ASTEX and the two GPCI columns.

Delivery date: 30 months

EUCLIPSE Description of Work: Deliverable 3.3

D3.3: Detailed analyses of the LES and SCM results for ASTEX and the two GPCI columns (Month 30).

Involved EUCLIPSE Partners: TUD, KNMI, MPG, METO, CNRS-IPSL, ECMWF, MF-CNRM, UW.

Aim

Large-eddy simulation and single-column models are used to study Lagrangian transitions of solid subtropical stratocumulus to shallow cumulus as the cloudy air mass is being advected towards the equator over increasingly higher sea surface temperatures. The simulations were carried out not only by all the relevant EUCLIPSE partners, but also by other participants from various weather and climate institutions as well as universities form outside the EUCLIPSE consortium.

The first case is based on observations collected during the ASTEX field campaign which allows to examine if models can faithfully represent the observed break-up of a solid stratocumulus cloud deck. Since it is found that LES models agree well with the observations, the range of large-scale forcing conditions that control the timing of the transition is broadened by adding three composite Lagrangian cases representative for the typical locations in the Eastern parts of the Pacific and Atlantic Ocean . In this way we can confront single-column model results with both observations and four high-resolution large-eddy simulation cases, each of which was forced by slightly different boundary conditions. We will particularly focus on the diurnal cycle of the cloud liquid water path and the timing of the break-up of the stratocumulus cloud deck. As this report describes the results of four Lagrangian transition cases in the Hadley cell, we decided to present the modelling results of the Eulerian experiments, i.e. low clouds at fixed points in the Hadley cell, in the report of D3.9.

1. Introduction

Low-level boundary-layer clouds occur frequently and persistently over the subtropical oceans. In general two dominant regimes can be distinguished; i) stratocumulus (StCu) and ii) fair-weather shallow cumulus (ShCu). While StCu is characterized by totally overcast conditions with high cloud condensate values, ShCu is characterized by low values of broken cloud cover consisting of an ensemble of optically thick shallow cumulus clouds. The StCu regime is located in the subsidence branch of the Hadley circulation where the lower-tropospheric stability is high, while the ShCu regime is situated further downstream in the low-level trade-wind flow where the stability is significantly weaker. At some point in the trajectory a transition from the one cloud type into the other takes place.

The striking difference in cloud structure of these two regimes is reflected in the associated impact on the vertical transfer of radiative energy through the atmosphere; the totally overcast and optically thick stratocumulus clouds are much more efficient in reflecting incoming shortwave radiation. Viewed from the perspective of numerical climate prediction, these differences in radiative forcing are significant. It is therefore important for General Circulation Models (GCMs) to correctly predict the properties of both cloud regimes as well

as their spatial distribution, in both present and future climate. A realistic representation of transitions from the one cloud regime to the other is an intrinsic part of this capability.

These arguments have motivated intense scientific research into low-level cloud transitions in the past, from which a conceptual picture has emerged that consists of the following sequence of events. First a thermodynamic decoupling takes place within the originally well-mixed boundary-layer (e.g. Wood and Bretherton, 2004), after which a shallow cumulus cloud base emerges below the capping StCu layer. Subsequently the boundary layer deepens, with the capping cloud layer thinning and eventually breaking up. The transitional situation, consisting of shallow cumuli rising into a capping cloud layer, is sometimes recognized as a separate cloud regime (e.g. Norris, 1998).

The time- and length-scales of the boundary-layer clouds involved in this transition are still much smaller than the discretization-sizes of numerical models applied in present-day weather- and climate prediction. Accordingly, in GCMs their representation is fully carried by parameterizations. The first GCSS inter-comparison study for Single-Column Models (SCM) on the StCu-ShCu cloud transition (Bretherton et al., 1999) revealed that while most codes reproduced a general deepening of the boundary layer, the performance was much worse concerning the cloud state during the transition. Considerable time has elapsed since this first intercomparison project, during which most BL schemes in operational weather and climate models have seen significant development. The question if this has led to a demonstrable improvement in the representation of clouds during the transition is still unanswered. This would justify revisiting the transition case. At the same time our understanding into the ``mechanics'' of the transition has progressed significantly. This has mainly been due to research based on field-campaigns and Large-Eddy Simulation (LES). Examples of improved insight include i) the process of decoupling during the transition, and the warming-deepening mechanism. One wonders if these important mechanisms are actually captured by the existing boundary-layer schemes, and if so, why.

This report aims to present a summary of the main results obtained in a new and recent inter-comparison project for LES and Single-Column Models (SCMs) on the StCu-ShCu transition that is designed to address these questions. The project is a joint activity of the GASS and the European Union Cloud Inter-comparison, Process Study and Evaluation Project (EUCLIPSE). While similarities exist between this inter-comparison project and the previous one presented by Bretherton et al. (1999), there are also important differences and key novelties. What both approaches share is their central goal of establishing model performance, and their use of LES results as reference in the evaluation of the SCM codes. A novelty is that simulations are now performed for four cases instead of one, each newly defined and each being somewhat different in configuration than the other. Expanding the evaluation from one to four cases spans a broader parameter space and thus aids the robustness of any conclusions. A second novelty is that the model performance for various key aspects of the transition is assessed using simple metrics, in order to clarify the presentation of model results and to objectively identify codes that yield promising results. A final novelty is that the model inter-comparison will focus on the representation of the newly discovered mechanisms as described above.

2. ASTEX LES results

2.1. Stratocumulus to shallow cumulus transition

Van der Dussen et al. (2012) compare LES results of a transition from a relatively well-mixed to a thin, decoupled stratocumulus layer with cumulus cloud penetration from below with

aircraft observations collected during the Atlantic Stratocumulus Transition Experiment (ASTEX). Figure 1 shows the lowest cloud base heights that are indicative of the lifting condensation level of the cumuli, in addition to the mean stratocumulus cloud base and cloud top heights. It can be seen that as the simulation progresses, the mean stratocumulus cloud base height keeps increasing, whereas the minimum cloud base height is approximately constant. The large separation between these heights in the second half of the simulation is indicative of the decoupling of the boundary layer and the development of saturated updrafts below the stratocumulus layer. The general picture of the transition is consistent in the models and in a close agreement with the observations which showed that after the second night the stratocumulus gradually broke up. The LES model results furthermore show that differences in the minimum cloud base height, which is indicative of lowest height where shallow cumulus clouds are present, are negligible small.

2.2. Entrainment and liquid water path

A plot of the entrainment rate w_e as a function of time is shown in Figure 2a, including estimates made on the basis of observations (De Roode and Duynkerke, 1997). The diurnal cycle is clearly visible in this plot, with significantly more entrainment during the night compared to daytime. The smaller entrainment rates during the day can be explained from the absorption of solar radiation in the cloud layer, which acts to stably stratify the cloud layer with respect to the underlying subcloud layer. Figure 2b shows the liquid water path (LWP). Estimates derived from the measured average liquid water specific humidity profiles are indicated by squares. During the night, the models show an increasing trend in the LWP. During early daytime, approximately 8 h after the start of the simulation, the LWP starts to decrease, to a local minimum approximately 2-3 hours after local noon. Even though the models agree on the bulk features of the transition, the spread in the LWP and the entrainment rate during the first 12 hours of the simulation is large. However, during daytime this spread is reduced significantly which can be explained by the fact that thicker clouds tend to absorb more solar radiation.

2.3. The effect of precipitation on the liquid water path

Figure 3a shows the LWP as a function of the precipitation rate at the stratocumulus cloud base. Both quantities are averaged over the first 12 hours of the transition. The top axis of the figure shows the LWP tendency due to precipitation. In addition to the reference case set-up, additional simulations were performed with DALES, using three different values of the cloud droplet concentration, namely 60, 100 (reference) and 200 cm^{-3}. In addition to the scheme by Khairoutdinov and Kogan (2000), which was used for the reference simulation, the simulations were also performed using the scheme of Seifert and Beheng (2001). The results strongly suggest that differences in the precipitation rates at cloud base explain the spread in the LWP, such as found in Figure 2b. Based on the LWP tendencies presented at the top x-axis of the figure, the expected LWP difference between for instance the UCLA LES and DALES results over the 12 hour period is approximately 250 gm^{-2}. Because the actual difference in the LWP at t=12 hr between these models is much smaller than this tendency suggests, some negative feedback mechanism must be present. Figure 3b clearly demonstrates that the entrainment rate decreases if the precipitation rate is higher. For the ASTEX case a smaller entrainment rate acts to reduce the drying at the top of the cloud, thereby counteracting the enhanced depletion of cloud water by precipitation (Ackerman et al., 2004). We also identify warming by solar radiation during daytime as an important feedback mechanism to reduce intermodel differences in the stratocumulus cloud thickness. Because thicker clouds absorb more solar radiation causing a larger thinning tendency, the LWP spread diminishes rapidly during the day.

Although the differences in the precipitation rates have a significant impact on the LWP

during the night, the fact that during daytime the LWP values tend to converge suggests that for the ASTEX case the details of the microphysics parametrization are of little importance to the timing of the stratocumulus cloud breakup.

2.4. Turbulence structure

Figure 4 demonstrates that the turbulence structure in the boundary layer as obtained from the LES models it is in a good agreement with the observations. The negative buoyancy flux at the top of the subcloud layer and the development of the double peaked vertical velocity variance profile is indicative of a decoupled cloud-top boundary layer, in which cumulus clouds grow from the top of the subcloud layer into the stratocumulus layer present under the inversion layer.

2.5. Vertical turbulent moisture transport

One of the objectives of the ASTEX field campaign was to determine the effect of the vertical transport of heat and moisture from the subcloud layer to the stratocumulus cloud layer by the cumulus clouds. Martin et al. (1995) and Wang and Lenschow (1995) suggested that in regions where cumulus clouds penetrate the cloud layer, the stratocumulus is thickened as the cumuli spread out into its base. Because the cumulus clouds have such an important impact on the maintenance of the stratocumulus cloud deck, we used the LES results to quantify which fraction of the surface evaporation is actually being transported out of the subcloud layer to the stratocumulus layer above. To this end we defined the flux ratio r_{qT} ,

$$r_{q_T} = \frac{\overline{w' q_T'}_{z_{sub}}}{\overline{w' q_T'}_0}$$

which quantifies the ratio of the vertical turbulent flux of the total water specific humidity at the top of the subcloud layer to its surface value. The flux ratio r_{qT} is presented in Figure 5 and shows a clear diurnal cycle. This indicates that during daytime moisture builds up in the subcloud layer and vice versa during nighttime. This is at a striking contrast with the buoyancy flux, which exhibits a nearly constant value at the top of the subcloud layer (De Roode et al. 2012).

The manuscript by Van der Dussen et al. (2012) presents a detailed analysis of the contribution of turbulent fluxes, radiation and precipitation to the LWP budget. Van der Dussen et al. (2012b) discuss sensitivity experiments with DALES, and show that smaller subsidence rates tend to cause deeper stratocumulus cloud layers and a longer persistence of the cloud layer.

3. Broadening the phase space: Composite Lagrangian cases

Sandu and Stevens (2011) present the setup of the 'Reference case', which is based on a composite of the large-scale conditions encountered along a set of individual trajectories performed for the northeastern Pacific during the summer months of 2006 and 2007. Both the initial profiles and the large-scale conditions represent the medians of the distributions of these various properties obtained from the European Centre for Medium-Range Weather Forecasts (ECMWF) Interim Re-Analysis (ERA-Interim) for the analyzed set of trajectories. For the study presented in this paper an additional ’Slow’ and ’Fast’ composite case are

proposed, each of which has a slightly different initial thermodynamic state. The initial vertical profiles of the liquid water potential temperature and total water specific humidity for the four different stratocumulus to shallow cumulus experiments are shown in Figure 6. The ASTEX case has the smallest value for the initial inversion jump in the liquid water potential temperature, which gradually increases in magnitude for the Fast, Reference and Slow cases, respectively. The inversion jumps in the total specific humidities are also different for each case, with the Slow case having the driest free atmosphere.

Figure 7 shows that the sea surface temperature (SST) increases with time for each case, which reflects the equatorwards lagrangian advection of the simulated air mass. For the ASTEX case the large-scale divergence gradually decreases with time, whereas a weakening of the wind velocities is taken into account by a time-varying geostrophic forcing. For the composite cases both the large-scale divergence and the geostrophic forcing are constant in time. Because the lower tropospheric stability is key for the evolution of the StCu to ShCu transition, a realistic tendency of the temperature is needed in particular as the simulations were performed for a period of two or three days. Therefore, for a faithfull representation of the radiative transfer in a cloudy atmosphere all models applied a full radiation code. The simulations lasted 72 hours, except for ASTEX which was simulated for 40 hours.

Figure 8a shows that for the three composite cases the LES models are rather well consistent in predicting the break-up and recovery of the stratocumulus. It appears that the LTS controls the dip in the cloud cover during daytime, with the 'Fast' case exhibiting the largest decrease. However, well before sunset the stratocumulus cloud deck recuperates with the cloud cover getting back to near unity values. Figure 8b shows that for the three composite cases the LWP increases the most during the night in the same models that showed a similar behavior as for the ASTEX case.

As a measure of the degree of decoupling De Roode et al. (2012) analyse the thermodynamic states of the subcloud and cloud layer for the liquid water potential temperature and the total water content. They find that for both quantities the difference between the two layer becomes larger for deeper boundary layers which is in agreement with observations reported by Wood and Bretherton (2004).

4. SCM results

Figure 9 evaluates the SCM results against LES for three cloud variables. The participating models are summarized in Table 2. For both LES and SCM the ensemble of models is plotted as a probability density function. A motivation for such ensemble-plotting is to clarify visualization, which gets complicated when the model ensemble contains a large number of codes. But perhaps the most important benefit of ensemble plotting is that it conveys how well the ensemble performs as a collective; it answers the question if common errors exist in the mean bias and time-development of the cloud transition. We find that in general the SCMs underestimate the rate of deepening of the boundary layer during the transition. What is also apparent is that considerable scatter still exists among the SCMs concerning the timing of the cloud break-up, a behaviour already established in the first intercomparison by Bretherton et al. (1999). In that sense not much improvement has been achieved since then. Finally, the variation in amplitude in the liquid water path during the transition is not well captured by the SCM ensemble, which fails to capture the transition from high values to low values as displayed by the LES ensemble. As will be discussed in the last part of this section, an individual assessment of the model skill to capture the transition suggests that relatively new or updated schemes tend to perform better.

A model may perform well in representing one aspect of the cloud transition, but less well for another. It is therefore interesting to search for an appropriate method to assess the overall performance of a model in representing the stratocumulus-to-cumulus transition. This may help in establishing which general approach in parameterization development is the most promising. To this purpose model performance is assessed for a chosen set of variables that reflect key aspects of the stratocumulus-to-cumulus transitions that we require the models to represent correctly. The set of nine state variables is listed in Table 3, including both vertically integrated properties as well as vertical structure. While most variables concern cloud state, some reflect the thermodynamic state of the boundary layer and its inversion.

The cumulative score for the set of nine variables is shown in Fig. 10, and is calculated as follows. The contribution for each variable can vary between 0 and 1, and is a linear function of the rank of each code as sorted on the distance between its position in bias-CRMS space and the origin (see Neggers, 2012). The best performing code (with the smallest distance) has the smallest contribution in the cumulative score. The summation of the contributions for all variables yields a single value that expresses the overall performance of the model relative to the other members of the ensemble for this particular set of variables.

An interesting result that can be interpreted from Fig. 10 is that the models making up the top-third of the list are generally those codes that are either i) entirely newly conceived concepts or are ii) existing schemes have seen significant renovation of their internal structure in recent years. What this suggests is that boundary-layer parameterization schemes that have some form of internal consistency between their individual components (such as thermodynamic transport, cloud macrophysics and microphysics) generally tend to do better for this type of cloud transition. An important reason could be that these type of internally consistent codes tend not to have a discretized configuration in which each cloud-regime has a different setting, but are formulated to be more generally and uniformly applicable to all regimes, including any transitions between them. The schemes thus respond smoothly to a smooth variation in the applied forcings, as is the case in the StCu to ShCu cloud transition.

5. Conclusions

Despite the complexity of the case and the long simulation period of 40 hours, the six participating state-of-the-art LES models faithfully represent the observed transition of a solid stratocumulus cloud deck to broken stratocumulus as observed during ASTEX. This case, and three composite Lagrangian cases demonstrate that that after some hours from sunset the stratocumulus cloud layer can become sufficiently thin leaving columns of clear air due to the absorption of solar radiation. The thinning rate appears to be related to the lower tropospheric stability (LTS) in the sense that the decrease in the cloud cover during daytime is larger for smaller LTS values. However, well before sunset the cloud cover and the stratocumulus LWP may increase again leaving a solid stratocumulus cloud deck during the night for all three composite cases. This recovery and thickening of the stratocumulus cloud deck can be partly explained from the radiative cooling of the cloud layer which is maximum during nighttime. However, also the moisture transported by the shallow cumulus exhibits a distinct diurnal cycle. In particular, during the night the cumuli transport significantly more moisture upwards than during daytime which supports a thickening of the stratocumulus cloud layer during the night.

The models are confronted with LES results for a chosen set of variables that reflect key aspects of the cloud transition. The obtained results for this set suggest that in general the SCM ensemble still has problems with various key aspects of this cloud transition, including the rate of deepening of the boundary layer, the timing of the cloud break-up, and the transition from high to low cloud integrated condensate loading. A positive result is that some

codes show promising overall results, which can possibly be attributed to a coherent and internally consistent approach in their boundary-layer parameterization schemes.

Bibliography

Ackerman, A. S., M. P. Kirkpatrick, D. E. Stevens, and O. B. Toon, 2004: The impact of humidity above stratiform clouds on indirect aerosol climate forcing, *Nature*, **432**,1014–1017.

Bretherton, C. S. , S. K. Krueger, M. C. Wyant, P. Bechtold , E. Van Meijgaard, B. Stevens, and J. Teixeira J, 1999: A GCSS boundary-layer cloud model intercomparison study of the first ASTEX Lagrangian experiment. *Bound.-Layer Meteor*., **93**, 341–380.

De Roode, S. R., and P. G. Duynkerke, 1997: Observed Lagrangian transition of stratocumulus into cumulus during ASTEX: Mean state and turbulence structure, *J. Atmos. Sci.,* **54**, 2157–2173.

Khairoutdinov, M., and Y. Kogan, 2000: A new cloud physics parameterization in a large-eddy simulation model of marine stratocumulus, *Mon. Wea. Rev*., **128**, 229–243.

Martin, G. M., D. W. Johnson, D. P. Rogers, P. R. Jonas, P. Minnis, D. A. Hegg, 1995: Observations of the interaction between cumulus clouds and warm stratocumulus clouds in the marine boundary layer during ASTEX. *J. Atmos. Sci.*, **52**, 2902–2922.

Norris, J. R., 1998: Low cloud type over the ocean from surface observations. Part II: Geographical and seasonal variations. *J. Climate*, **11**, 383-403.

Sandu, I. and B. Stevens, 2011: On the factors modulating the stratocumulus to cumulus transitions. *J. Atmos. Sci.,* **68**, 1865–1881.

Seifert, A., and K. D. Beheng, 2001: A double-moment parameterization for simulating autoconversion, accretion and selfcollection, *Atmos. Res*., **59-60**, 265–281.

Wang, Q., D. H. Lenschow, 1995: An observational study of the role of penetrating cumulus in a marine stratocumulus-topped boundary layer. *J. Atmos. Sci*., **52**, 2778–2787.

Wood, R., and C. Bretherton, 2004: Boundary layer depth, entrainment, and decoupling in the cloud-capped subtropical and tropical marine boundary layer. *J. Climate*, **17**, 3576-3588.

Output

Model data

Table 1 summarizes the LES models that participated in the ASTEX and three composite intercomparison cases. The ASTEX results that are discussed by van der Dussen et al. (2012) can be downloaded from http://www.euclipse.nl/wp3/LES_Data/ASTEX/

Investigator	LES model	Institution
A. Ackerman	DHARMA	NASA, Goddard Institute for Space Studies (GISS), New York, USA
P. Blossey	SAM	University of Washington, Seattle, USA
M. Kurowski	EULAG	University of Warsaw, Warsaw, Poland
A. Lock	MOLEM	Met Office, Exeter, UK
I. Sandu	UCLA-LES	Max-Planck Institut für Meteorologie (MPI-H), Hamburg, Germany
J. van der Dussen	DALES	Delft University of Technology, Delft, The Netherlands

Table 1: List of LES models participating.

An online interface for the interactive visualization of model results for this inter-comparison case was launched as part of this project. The website can be found at http://www.knmi.nl/samenw/rico/RICO/. It consists of an online plotting tool that is coupled to a database of both SCM (see list of participating models in Table 2) and LES results for this case. Participants can use this tool to compare their SCM results to others, using various plotting methods. In addition, results for previous inter-comparison cases are also posted on the website, which can thus start to function as an archive for SCM evaluation for use by the modelling community. We hope that this may serve and assist in further model development and improvement in the future.

Investigator	SCM	Institution
E. Basile	AROME	Météo France
	ARPEGE-NWP	
I. Beau	ARPEGE-CLIMAT	Météo France
V. Larson	CLUBB	UWM
S. dal Gesso,	EC-Earth,	KNMI
R. Neggers	RACMO	
S. Kumar	ECHAM6	MPI-M Hamburg
I. Sandu	IFS cy36r1	ECMWF
M. Köhler		
H. Kawai	JMA	JMA
A. Cheng	LaRC	NASA LaRC
H. Xiao	UCLA-AGCM	UCLA
M.-P. Lefebvre	LMDZ	IPSL
W. Angevine	WRF TEMF	NOAA
C. de Bruijn	HARMONIE EDKF,	KNMI
W. de Rooij	HARMONIE EDMF	
J. Fletcher	NCEP GFS	University of Washington
S. Park	NCAR CAM5	University of Washington
I. Boutle	UKMO	UK Met Office

Table 2. List of participants in the SCM inter-comparison study, their affiliation, and the name of the model code.

Variable	*Acronym*	*Units*	*Description*
Total Cloud Cover	TCC	%	Vertically projected area covered by clouds
Liquid water path	LWP	g m^{-2}	Vertically integrated liquid water
Cloud top height	z_{top}	km	
Cloud base height	z_{base}	km	
Height of 1st maximum in cloud fraction	z_{max}^{1st}	km	
Height of 2nd maximum in cloud fraction	z_{max}^{2nd}	km	
Depth of capping cloud layer	Δz_{cap}	km	
Decoupling parameter	α	-	The difference In total specific humidity between the mixed=layer and cloud layer, normalized by the mixed layer humidity (Wood and Bretherton, 2004)
Cloud top entrainment instability parameter	κ	-	Ratio of the temperature jump to the humidity jump across the boundary-layer inversion (Kuo and Schubert, 1988)

Table 3. The set of nine variables used for evaluation of the SCMs.

Documents

Neggers, R.A.J., EUCLIPSE WP3 progress report - SCM case studies
http://www.euclipse.eu/Publications_new.html)

van der Dussen, J. J. , S. R. de Roode, A. S. Ackerman, P. N. Blossey, C. S. Bretherton, M. J. Kurowski, A. P. Lock, R. A. J. Neggers, I. Sandu, and A. P. Siebesma, 2012: The GASS/EUCLIPSE Model Intercomparison of the Stratocumulus Transition as Observed During ASTEX: LES results. Submitted to the *J. Adv. Model. Earth Syst., (see http://www.euclipse.eu/Publications_new.html)*

Van der Dussen, J, S. R. de Roode and A. P. Siebesma, 2012b: LES sensitivity experiments of the EUCLIPSE stratocumulus to cumulus transition based on ASTEX. *20th Symposium on Boundary Layers and Turbulence*, 9-13 July 2012, Boston, MA, USA *http://www.euclipse.eu/Publications_new.html)*

de Roode, S. R., I. Sandu, J. van der Dussen, A. S. Ackerman, P. N. Blossey, A. Lock, A. P. Siebesma, and B. Stevens, LES results of the EUCLIPSE Lagrangian stratocumulus to shallow cumulus transition cases. *20th Symposium on Boundary Layers and Turbulence,* 9-13 July 2012, Boston, MA, USA
http://www.euclipse.eu/Publications_new.html)

Figures

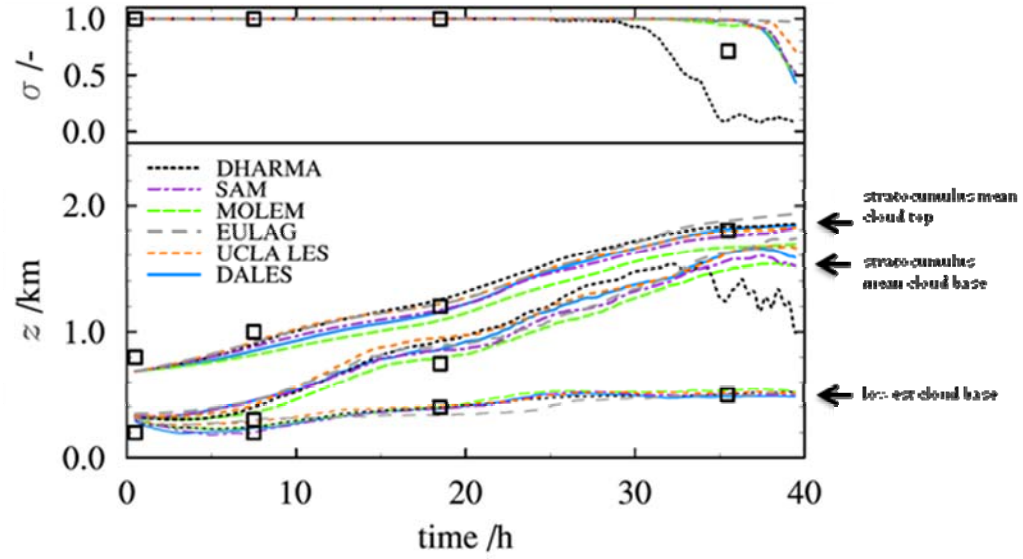

Figure 1. The total cloud cover σ (top panel) and the contours of the simulated clouds (bottom panel) composed of the inversion height (as an indication of the mean stratocumulus cloud top), the minimum cloud base height and the mean cloud base height, for each of the models shown in the legend. The squares denote similar quantities, estimated from the profiles of the observed liquid water content.

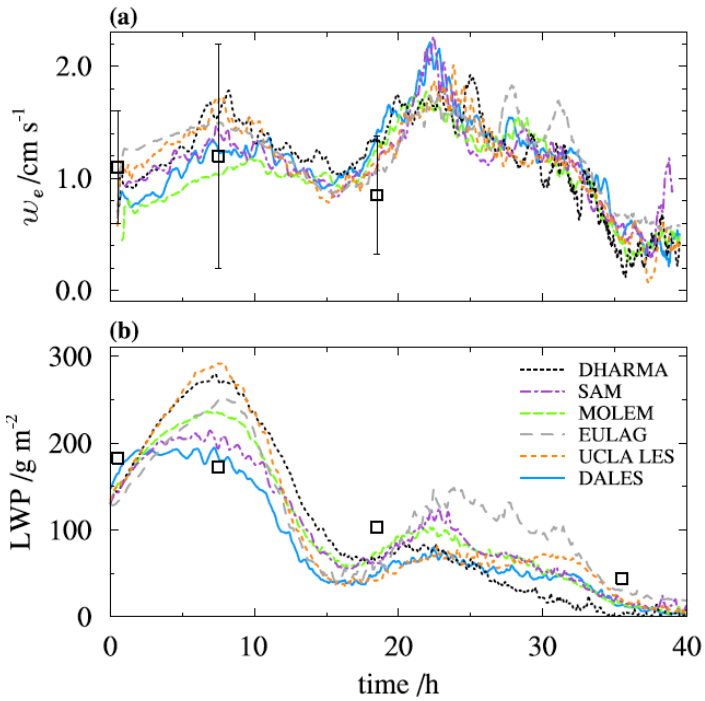

Figure 2. The entrainment rate w_e (a) and the liquid water path LWP (b) as a function of time for the models indicated in the legend. Estimates based on observations of w_e, including uncertainties were obtained from De Roode and Duynkerke (1997), while the values of the LWP where obtained by integrating the mean liquid water content profiles. A running averaging filter with a width of 1 h has been applied on the entrainment rates from the simulations.

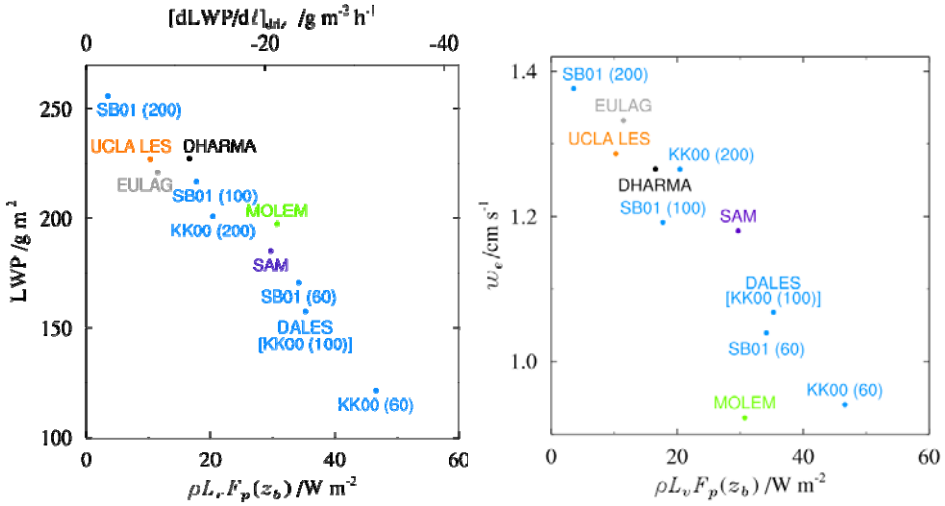

Figure 3. Scatter plots of the time averaged (left panel) LWP and entrainment rate (right panel) as a function of time averaged precipitation rate at stratocumulus cloud base. Each quantity is averaged over the first 12 hours of the simulation. The top axis shows the precipitation rate in terms of a LWP tendency in $gm^{-2}\ h^{-1}$. The labels indicate the model or the microphysics scheme (in DALES) used, while the numbers between the parentheses indicate the cloud droplet number density in cm^{-3}.

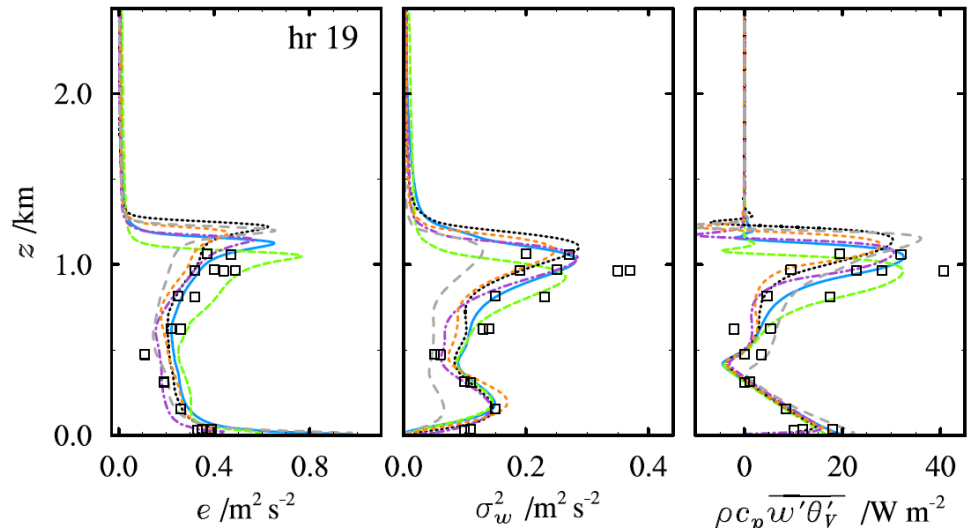

Figure 4. Turbulence vertical profiles from the LES models and aircraft observations for the turbulent kinetic energy (e), the vertical velocity variance (σ_w^2), and the virtual potential temperature flux during the 19th hour of the simulation.

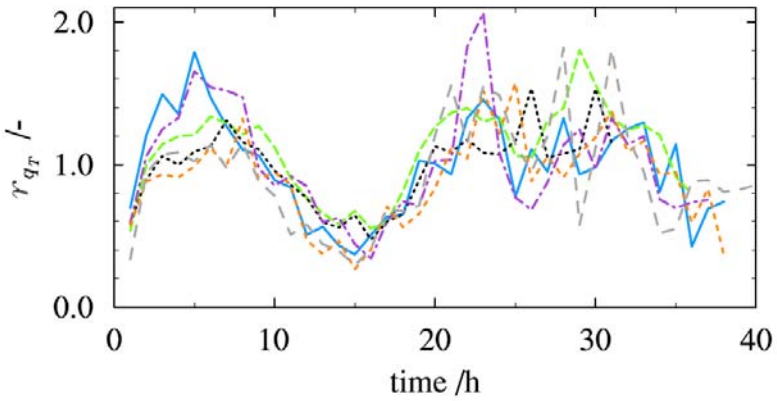

Figure 5. The factor r_{qT}, which is defined by the moisture flux at the top of the cloud base normalized by its surface value.

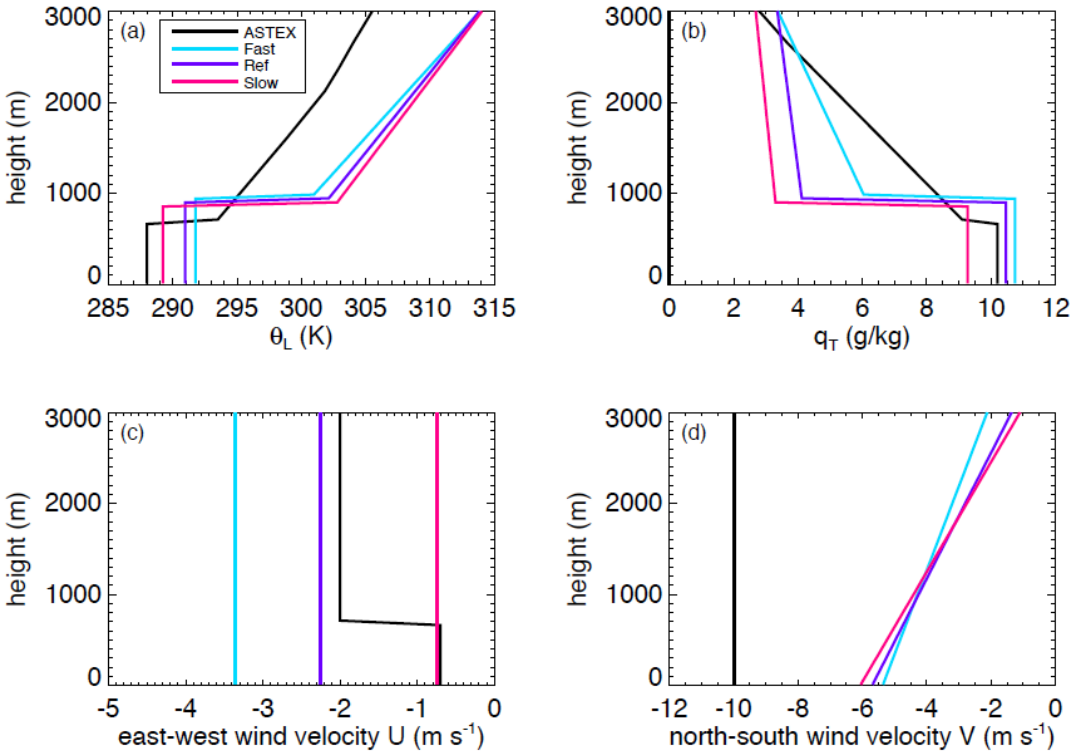

Figure 6: Vertical profiles of the initial liquid water potential temperature θ_L, total water content q_T, and the horizontal wind velocity components U and V for the ASTEX, Fast, Reference and Slow cases. The line styles are according to the legend.

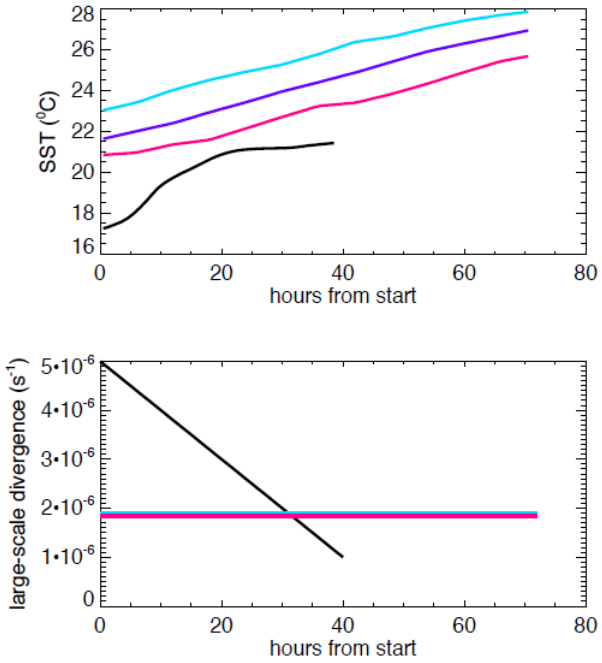

Figure 7: Prescribed sea surface temperature and large-scale divergence as a function of time for the four stratocumulus to shallow cumulus transition cases. The linestyles are the same as in Figure 6.

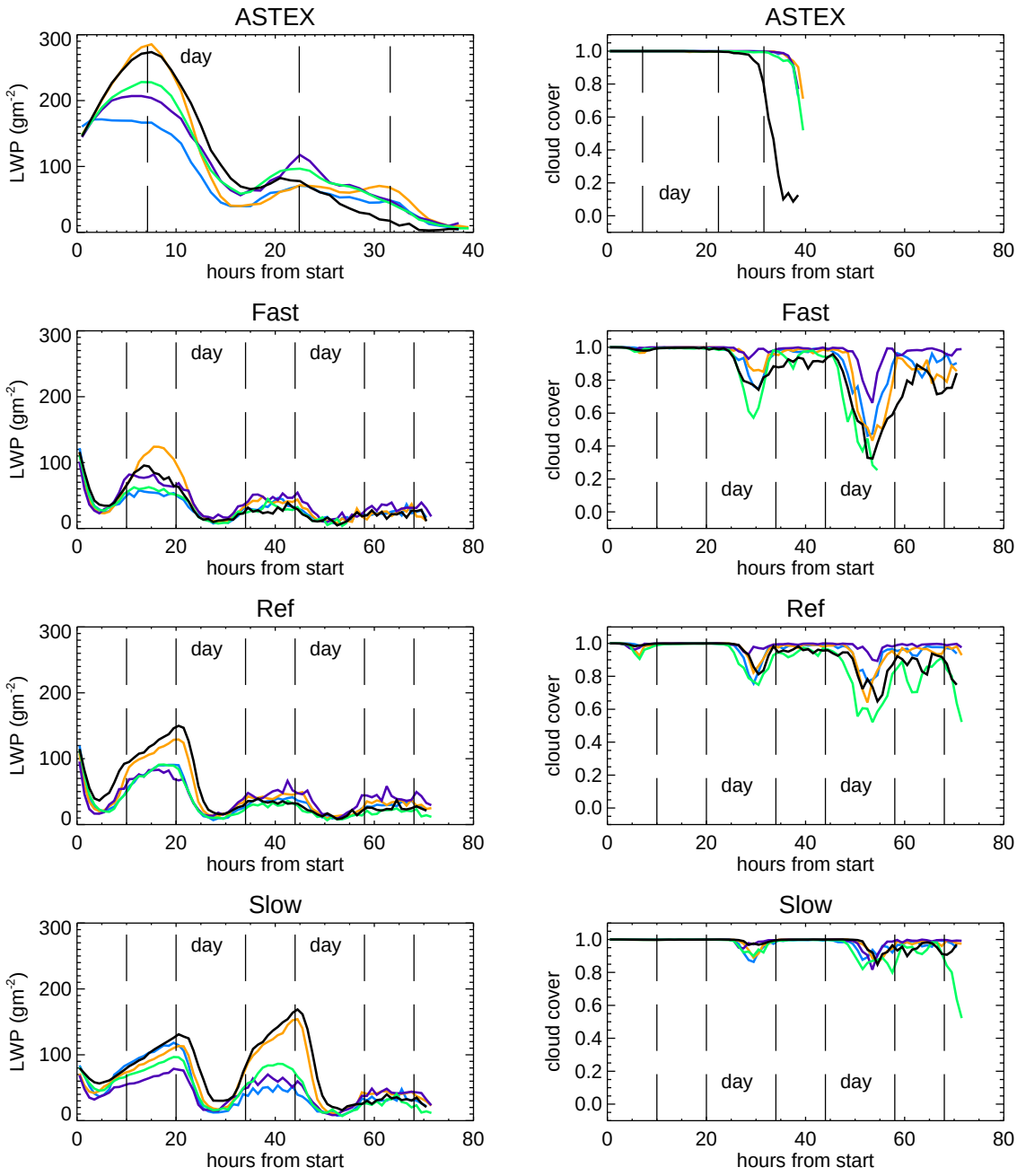

FIGure 8: LES results of the cloud cover (left) and the liquid water path (LWP, right) for the ASTEX, Fast, Reference and Slow cases. The line colors are as in Figure 1.

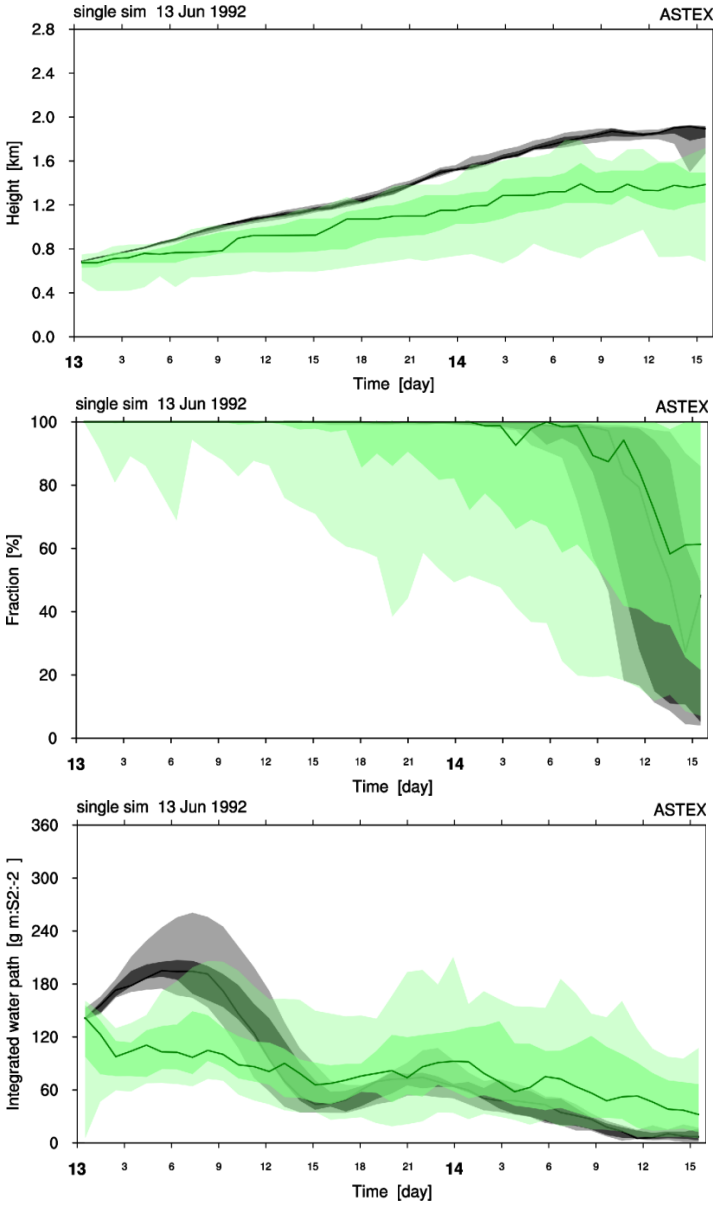

Figure 9. Time-series of the liquid water path during the cloud transition in the ASTEX case. The ensemble of LES models is shown in grey, while the SCM ensemble is shown in green. In both distributions the 50 percentiles (the median) is indicated by the solid line. The areas of different shading correspond to various percentiles of the distribution; the part of the PDF between the 5-95 percentile is lightly shaded, while that between the 25-75 percentiles in densily shaded.

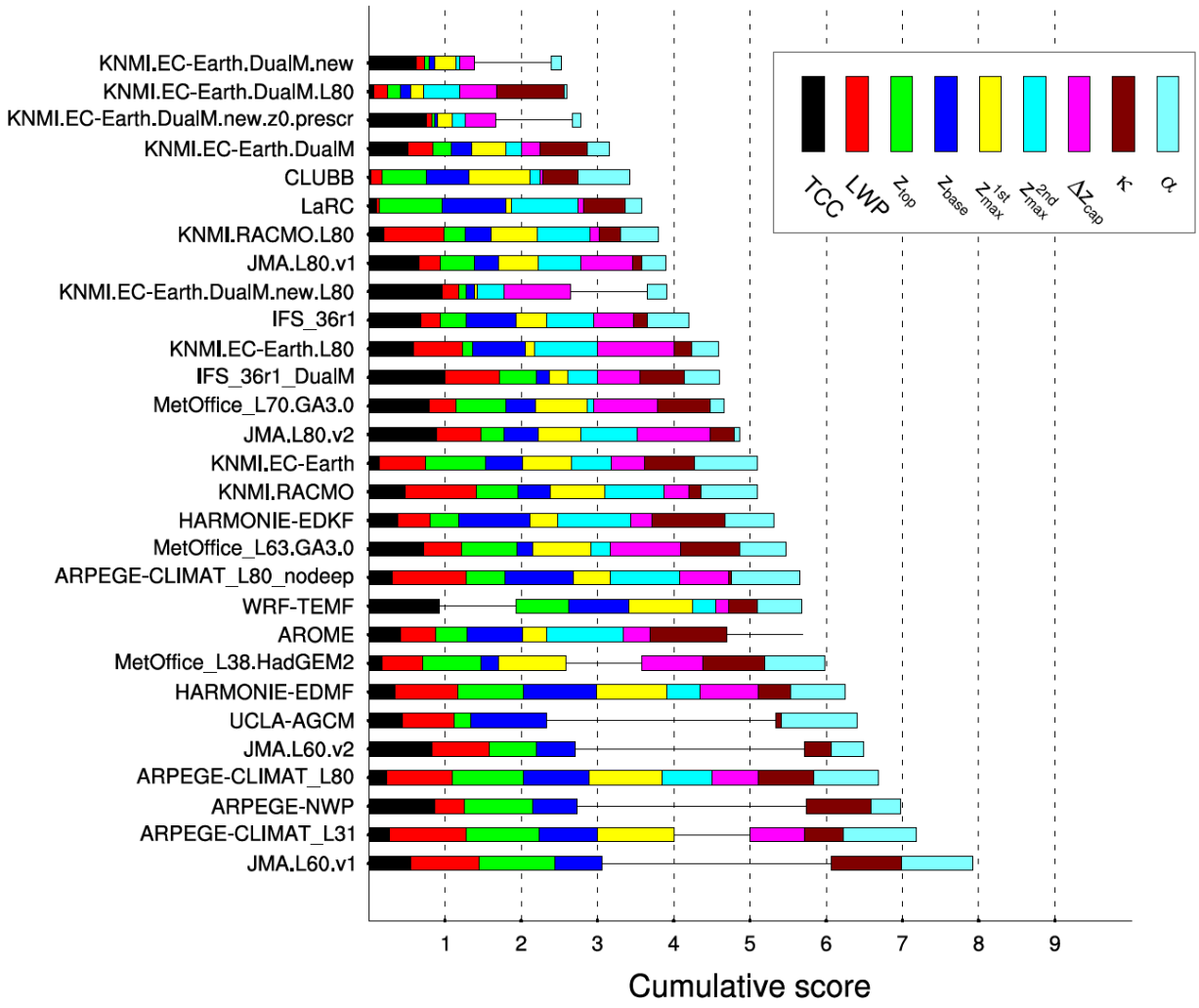

Figure 10. Bar-chart showing cumulative model performance estimated over nine variables according to Table 3 reflecting key aspects of the cloud transition. The colors indicate the contribution to the cumulative score by individual variables, as explained in the legend. The models on the vertical axis are sorted on their cumulative scores, with the best performing model (lowest cumulative score) positioned at the top. In case the model output on a certain variable is unavailable, the contribution is assumed equal to 1 and is shown as a solid horizontal line.